Erbium-doped Fiber Amplifiers Design Strategies to Optimize Capacity in Submarine Systems

Juliana Tiburcio de Araujo[a], Alberto Bononi[b], Jean-Christophe Antona[a], Alexis Carbo Meseguer[a], and Christian Simonneau[a]

[a]Alcatel Submarine Networks, Nokia Paris-Saclay, Nozay, France
[b]Dipartimento di Ingegneria e Architettura, Università di Parma, Parma, Italy

ABSTRACT

We revisit the design strategies of erbium-doped fiber amplifiers (EDFA) in wavelength division multiplexing (WDM) submarine links over transoceanic distances. We particularly investigate the optimization of EDFA settings such as fiber length, optical bandwidth and population inversion to maximize the power efficiency and/or achievable information rate (AIR) at fixed span length. When optical bandwidth is fixed, we show the existence of a unique EDFA optimum setting whatever the pump power, provided Kerr-effect is overlooked. When accounting for Kerr-effect, the EDFA parameters can be adjusted to improve AIR as pump power increases. We also show a performance enhancement when working with a variable bandwidth design at very-low and very-high pump powers.

Keywords: erbium-doped fiber amplifiers, spatial division multiplexing, submarine optical networks, nonlinear fiber optics, coherent systems

1. INTRODUCTION

Information traffic demand has grown significantly over the past decades and continues to grow at a high pace.[1] Historically, several technological advancements enabled optical fiber networks to cope with this high demand. The introduction of WDM, mainly due to the development of EDFAs, permitted the simultaneous transmission of several modulated channels in a single fiber by optically combining them in the frequency domain. It allowed the channel wavelength separation to be as small as a fraction of a nanometer, drastically increasing the system's spectral occupancy. Besides, with the advent of coherent detection, transceivers became rate-adaptive, software-defined, and able to transmit channels with possibly different performances. Moreover, information could be modulated using multiple degrees of freedom, such as amplitude, phase and polarization, allowing high spectral efficiency. It gave rise to polarization division multiplexing and phase/amplitude modulation formats, as well as enabled the electronic compensation of some link impairments, such as chromatic dispersion and self-phase modulation (SPM), with digital signal processing. In addition, systems also improved the quality of transmission by implementing forward error correction to minimize bit-error rate, and evolved to generate more advanced modulation formats, such as probabilistic constellation shaping, approaching Shannon's limit of capacity.

Thus, prior submarine cables used to operate at low fiber count and at the optimal electrical signal-to-noise ratio (SNR) per fiber. However, subsea systems face another intrinsic limitation in terms of power feeding, the high voltage of cable extremities, typically up to 15-18 kV: in case an electrical defect arises along the cable and the conductor is in contact with water, then for a short period of time, the high voltage difference at conductor–sea interface will give rise to very high surges of electrical current, possibly damaging all components along the cable. Therefore, increasing cable powering through higher voltages in order to feed more repeaters with more parallel fibers is far from being an easy path and requires to ensure all components of the cable are resistant enough to such electrical current surges. Then long or high fiber count cables will result in lower available pump and optical output powers per amplifier and consequently, the fiber throughput capacity. A solution to increase the system performance given this energy constraint came from the Shannon formula, which shows a logarithmic scaling of the total capacity with SNR while a linear scaling with the degree of parallelism.

Further author information: J. T. A.: E-mail: juliana.tiburcio_de_araujo@asn.com

Hence, the strategy of maximizing the capacity per fiber by operating each fiber at top SNR was replaced by maximizing the total cable capacity with a higher number of fiber pairs (FP), all with lower power per fiber, while ensuring that the available electrical power per repeater is efficiently shared to feed a high fiber count. This was the beginning of spatial division multiplexing (SDM) implemented in nowadays systems, in which the number of spatial paths is more explored, reaching up to 24 FP in one cable. SDM systems were enabled by the pumping sharing technique, leveraging the optical combination of high power 980 nm amplifier pumps (thus operated at high power efficiency), then its optical coupling to feed a high count of optical amplifiers, resulting in energy-efficient, possibly low optical pump powers multiplexed into amplifiers. Although this solution enabled to improve the repeater's power efficiency (PE),[2] power limitation is still the factor that most limits the capacity of current systems, showing the need of improving the amplifier's optical PE.[3]

To include power constraints in the system design, different definitions of PE were introduced. Sinkin *et al.* defined in Ref. 4 $PE_S \triangleq AIR/P_O$, where P_O is the amplifier optical output power. Lately, Downie *et al.* proposed in Ref. 5 $PE_D \triangleq AIR/P_p$, being P_p the optical pump power at each amplifier. This definition comes from the assumption that P_p would be a better representation of the electrical power consumption than P_O, since amplifiers output power typically follows an affine law with pump power in similar population inversion conditions, which depends on the transparency pump - power in which the amplifier starts to emit photons.[6] By considering P_O in the PE definition, one neglects the contribution of the transparency pump, making the power efficiency prediction less accurate. It has been shown in Ref. 7 that PE_D provides a better agreement with experimental results than PE_S.

Another important concept to accurately assess systems' PE is the signal and noise droop.[8,9] At low-SNR regimes, the inverse SNR noise accumulation to compute the generalized-SNR is no longer valid and the Generalized Droop (GD) Formula must be applied.[10] This effect comes from the fact that in subsea systems, amplifiers operate in constant output power (COP) mode, preserving the same total output power (and spectrum) after the gain shaping filter (GSF) of each amplifier. However, noise power, as amplified spontaneous emission (ASE), accumulates with the distance, making the signal (and the existing noise before the amplifier) to deplete in order to maintain a COP. By accounting for signal droop, we can find an optimal SNR that maximizes PE around 0 dB, showing that there is a fundamental limit for parallelism of SDM systems.

Then, using the PE metrics and GD model, several studies[5,11–14] addressed the power limitation problem and sought to improve the PE of a system's single spatial path by optimizing different amplifier degrees of freedom, such as the optical bandwidth (BW), the gain shaping filters and the input power allocation. In particular, Perin *et al.* showed the importance of using physical EDFA models to optimize capacity of power-constrained systems.[11] Complementary to these previous investigations, we revisit different EDFA optimization strategies following the theory developed in Refs. 13, 14, which is based on Saleh amplifier model – a closed-form expression of the Giles-Desurvire rate equations at steady state. In particular, we numerically search for the amplifier parameters length and population inversion that enable to reach the maximum AIR at each pump power.

In this study, we consider two different scenarios for a given transmission link (distance, amplifier gain, fiber type): a fixed 5 THz bandwidth in the C-band and a variable BW up to 5 THz (since EDFAs in subsea links are currently limited to this BW). By fixing the bandwidth, we show a single EDFA length and inversion that maximizes AIR at each pump power when nonlinear interference (NLI) is overlooked. Besides, we also show that optimizing population inversion is responsible for a continuous increase of AIR with pump power even when accounting for NLI. These results were not evidenced in prior work because they always worked with an unconstrained BW. Moreover, we extend the analysis to very low and very high pump powers and compare the optimal design with simpler strategies, quantifying the gain in PE/AIR and discussing their feasibility in power-constrained subsea systems. This paper also allows to show the evolution of both system and EDFA's optimized parameters with pump power within different scenarios, as well as to consolidate prior studies by showing coherent results, such as the growth of optimal bandwidth with pump power, as in Ref. 5, and the saturation of optimal launch power at high pumps, as in Ref. 11.

2. LINK AND MODELS DESCRIPTION

We consider a WDM transmission on a single spatial path along a homogeneous link with fixed span loss ($A > 1$), identical end-span EDFAs and all with optical pump power P_p. The N_c WDM channels are launched into all

EDFAs with a constant input power (CIP) over spectrum and the GSF after each EDFA keeps the spectrum flat at the output of each span, yielding a so-called constant power spectral density (CPSD) line.[13,14]

The received SNR after M spans at a generic channel j is obtained from the Generalized Droop formula[8,10] as: $\mathrm{SNR}_j = (\chi_j^{-M} - 1)^{-1}$, where $\chi_j = (1+\mathrm{SNR}_{1j}^{-1})^{-1}$ is the signal droop per span[10] and $\mathrm{SNR}_{1j} = (\frac{\delta Q_{rj}}{Q_j} + \frac{\delta Q_{aj}}{Q_j} A)^{-1}$. The depletion of signal power (droop) occurs in order to maintain a CPSD span after span, since noise power accumulates over the distance. Here, for each channel j, Q_j is the transmitted flux, δQ_{rj} the nonlinear span-generated interference flux, and δQ_{aj} the input-equivalent ASE flux generated at the end-span EDFA. Then, the AIR per 2-polarization spatial path is given by:

$$\mathrm{AIR} = \sum_{j=1}^{N_c} 2\Delta f \log_2(1 + \Gamma \mathrm{SNR}_j) \tag{1}$$

where Γ is the SNR gap to capacity and Δf is the channel bandwidth. The NLI flux δQ_{rj}, which includes cross-channel interference (XCI) and self-channel interference (SCI), is calculated as in Ref. 14 by using the Gaussian Noise (GN) model.[15]

For the EDFA, we use the Saleh model extended to include ASE self-saturation.[13,16] Instead of solving the Giles-Desurvire rate equations, this model relies on a closed-form expression of the forward and backward ASE by using a good[16] constant inversion approximation over the EDF length. In the steady-state, the flux balance equation is given by: $\sum_{j=1}^{N_c} \frac{Q_j}{A}(G_j(x) - 1) = \kappa(x, Q_p)$, with $G_j(x) = \exp(L(\alpha_j + g_j^*)x - \alpha_j)$ the EDFA gain, x the population inversion, L the length, g_j^* and α_j the Giles emission and absorption parameters.[17] $\kappa(x, Q_p) = Q_p(1 - G_p(x)) - \frac{r_M}{\tau}x - Q_{ASE}^{F+B}(x)$ is the useful pump flux, with Q_p the pump flux, G_p the pump gain, τ the fluorescence time, r_M the total number of erbium ions and $Q_{ASE}^{F+B}(x)$ the ASE forward and backward flux. The EDFA noise figure at channel j is: $F_j = 2n_{sp,j}(x)\frac{G_j - 1(x)}{G_j(x)}$, where $n_{sp,j}(x)$ is the spontaneous emission factor.

Using the extended Saleh model described above, it is shown in Ref. 13 that the input flux that maximizes AIR for a given EDFA gain and pump power for the CIP channel allocation is:

$$Q_j = \frac{\kappa(x, Q_p)\frac{1}{f_j}}{\sum_{i=1}^{N_c} \frac{1}{Af_i}(G_i(x) - 1)} \tag{2}$$

where f_j is the frequency of channel j. It is also reported in Ref. 13 that CIP allocation is quasi-optimal when x is optimized, making our flat input power a reasonable assumption. Since both the bandwidth and the optimal input power may vary with the EDFA gain, which in turn is a function of the EDFA length and inversion, then the maximum AIR is highly dependent on these parameters. Therefore, we have a major interest to optimize x and L and quantify the gain in AIR that it provides.

When the EDFA inversion is fixed, its gain shape is also fixed, then the EDFA+GSF total output power P_O follows a simple affine-law as a function of P_p:[6,8]

$$P_O = \begin{cases} \eta_{oo}(P_p - P_{p0}), & \text{if } P_p \geq P_{p0} \\ 0 & \text{else} \end{cases} \tag{3}$$

being P_{p0} the transparency pump and η_{oo} the optical-to-optical conversion efficiency. Here, h is the Planck constant and f_p is the pump frequency. We show in Appendix A that P_{p0} and η_{oo} are related to the EDFA physical parameters by the following expressions for a CIP input:

$$P_{p0} \triangleq \frac{hf_p(\frac{r_M}{\tau}x + Q_{ASE}^{F+B}(x))}{1 - G_p(x)} \tag{4}$$

$$\eta_{oo} = \left(\frac{N_c A \frac{(1-G_p(x))}{hf_p}}{\sum_{j=1}^{N_c} \frac{G_j(x)-1}{hf_j}} \right) \tag{5}$$

3. SCOPE OF WORK

We studied a link with CIP allocation (flat input spectrum) with the following parameters, similar to Refs. 11, 14: single mode fiber (SMF) attenuation of 0.162 dB/km, chromatic dispersion of 21 ps/nm/km, effective area of 130 μm^2, 2 dB gap to capacity, a flat per-span attenuation of 9.5 dB, in which 9 dB is due to span loss and 0.5 dB is added as margin, leading to a span length of 55.5 km. We investigate links with 100, 200 and 300 spans, which are typical distances of subsea networks. The channels are centered at frequency bins spaced by 50 GHz, which launch power is optimized to reach maximum AIR according to eq. (2). We suppose that 50% of self-phase modulation (SPM) is compensated at the receiver to emulate the nonlinear compensation (NLC) in coherent detectors. EDFA emission and absorption cross sections and other relevant parameters such as erbium concentration and doped-fiber core area used are the same as reported in Ref. 11.

In that context, we performed a numerical search to find the EDFA population inversion and length that maximize AIR at different pump powers, considering two cases. In the first case (that we will call *fixed* BW), we fix the used optical bandwidth to 5 THz in the C-band ([1528-1568] nm) by restricting the search only to pairs (x, L) that yield a gain above span loss over the entire C-band, such that all the 100 channels in the C-band are occupied. In the second case (that we will call *variable* BW), we allow the BW to vary and possibly be lower than 5 THz, hence without constraints on the (x, L) pair. We assess the system performance in the two cases by computing the AIR and the PE, defined as in Ref. 5: PE $\triangleq \frac{\text{AIR}}{P_p}$, where we recall that P_p is the *optical* pump power at each EDFA.

In both cases, we also show the performance of two simpler EDFA design strategies: when only the inversion is optimized at each pump power (but length is fixed), and when both x and L are fixed (hence BW is also fixed). In the following, these designs will be labeled respectively as (x_o, L_f) and (x_f, L_f), where the sub-index 'o' stands for optimum and 'f' for fixed. The fixed values for length and inversion are the optimum ones (maximizing AIR) at a reference pump power without NLI. We chose a reference pump of 20.8 dBm (120 mW), which permits to operate the fixed-BW system at nonlinear threshold (NLT) for a 300-span link without NLC.

Given their simplicity compared to the optimal design, (x_f, L_f) and (x_o, L_f) are interesting when performing laboratory parametric experiments with the same EDFA equipment. By fixing the length and inversion, the same EDFA and GSF can be used to perform transmission experiments independently of the pump power, which is possible by adjusting the amplifier output power accordingly with the pump. In addition, in this case, we are within the affine law assumptions, hence we can use it to model the EDFA. Because of the affine law simplicity compared to EDFA physical models, it is preferable to use the first one to perform wide-scale and quick parametric studies, as it was done in Ref. 18. With this simple model, we only need to know the optical-to-optical conversion efficiency and the transparency pump that can be easily characterized experimentally or computed from the Saleh model once for all pumps (eqs. (4) and (5)). In addition, physical models also have the disadvantage of needing input EDFA parameters that are not readily available for commercial EDFAs, such as the Giles parameters. Finally, the (x_o, L_f) strategy can also be interesting for laboratory experiments, since at fixed L we can manage to change the amplifier inversion by varying its input power. We can, therefore, use the same amplifiers for all pump powers, provided we can adjust the GSF (e.g. by the use of programmable filters such as Wavelength Selective Switches to correct the usual fixed filters used as GSF, or to replace them).

4. NUMERICAL RESULTS

4.1 Fixed Bandwidth (5 THz)

Figs. 1 and 2 show, respectively, the PE and AIR versus P_p for different strategies, for a 100, 200 and 300-span link, a fully occupied C-band, with and without NLI. PE figures mainly matter for optimizing power-constrained subsea systems where cable AIR optimization at fixed total pump power budget results in high fiber count with low optical pump per amplifier. Conversely, when powering is not an issue, fiber AIR optimization may be considered as in the era of the pre-SDM subsea systems.

In Figs. 1 and 2, solid, dashed and dotted lines correspond, respectively, to (x_o, L_o), (x_o, L_f) and (x_f, L_f) designs, and different colors are associated to the different distances. Inset in Fig. 1(b) zooms the results for P_p ranging from 25 to 30 dBm. Vertical solid lines in Figs. 1(a) and 2(b) indicate the nonlinear threshold (NLT), defined as the pump power at which AIR is maximized when operating in (x_f, L_f) mode. The amplifier total output power at NLT for [100, 200, 300] spans is, respectively: [18.9, 18.8, 18.7] dBm, corresponding to pump powers of [22.4, 22.3, 22.2] dBm. Dashed-dotted vertical lines indicate the reference pump power (20.8 dBm), used to set the (x_f, L_f) values at each distance. We recall that this reference pump allows the 300-span link to operate at NLT when NLI is not compensated. In this fixed-BW case, the corresponding values of (x_f, L_f) for 100, 200 and 300 spans are all equal to (0.627, 6.5 m). Finally, the figures also show, in symbols, the perfect match between the affine law and the results of the Saleh model for the (x_f, L_f) strategy.

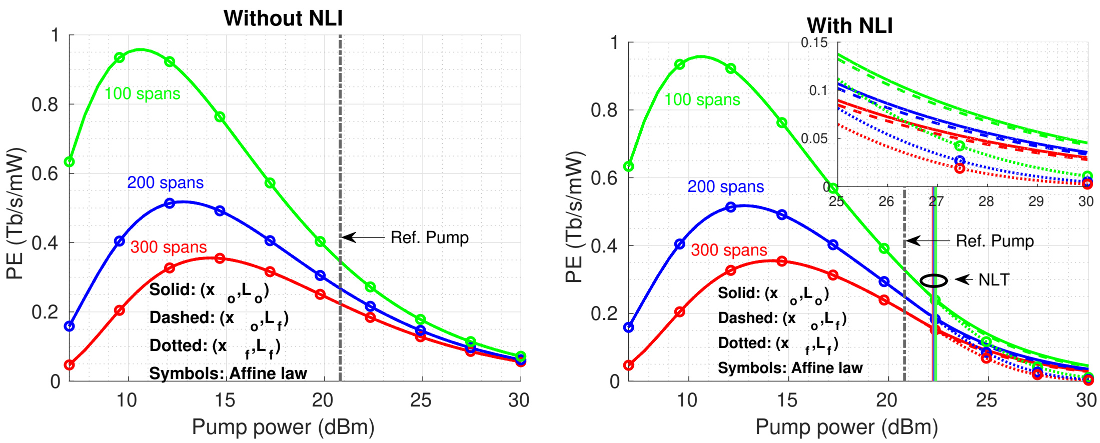

(a) (b)

Figure 1. Power efficiency versus pump power for the different optimization strategies and distances, with a fixed 5 THz bandwidth and a) without NLI and b) with NLI. Inset is a zoom of PE from 25 to 30 dBm pump power. Symbols are the (x_f, L_f) strategy results reproduced with the affine-law.

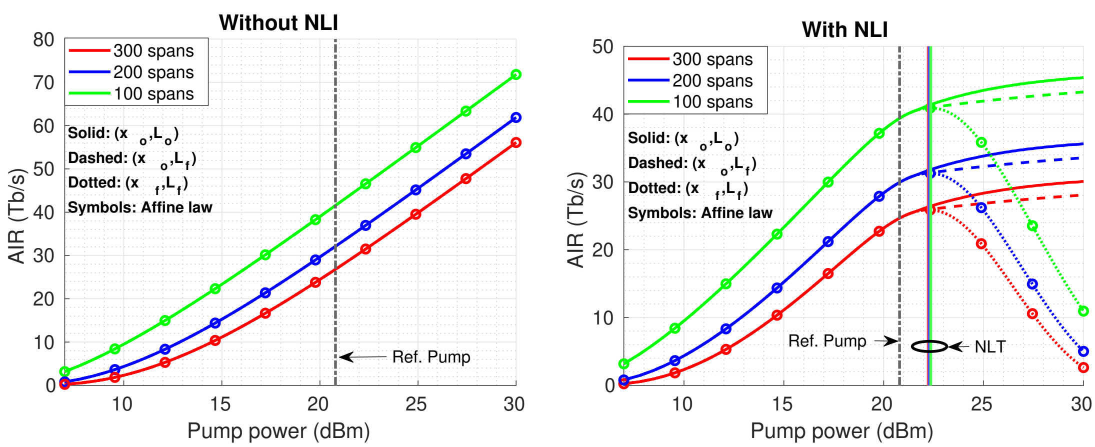

(a) (b)

Figure 2. Achievable information rate versus pump power for the different optimization strategies and distances, with a fixed 5 THz bandwidth and a) without NLI and b) with NLI. Symbols are the (x_f, L_f) strategy results reproduced with the affine-law.

From the figures, we see that all designs coincide at low pumps, but start to diverge at the highest pumps only when including nonlinearities. In the linear regime or at low pumps, this means that, if we target a minimum gain level with a certain bandwidth, we have a unique simple amplifier design that also allows us to use the affine law (eq. (3)) to simply model the EDFA.

In presence of NLI, the gain in PE when using (x_o, L_o) compared to (x_f, L_f) design represents only $[1.2, 1.5, 1.6]\%$ at the corresponding NLT for each distance, but continues to increase as pump power grows. For comparison, with 0% and 100% of NLC the gain would be respectively of $[2.2, 2.8, 3.3]\%$ and $[0.2, 0.1, 0.1]\%$ for a [100, 200, 300] spans link at the same pump power. The increase of the PE gain with P_p when usign (x_o, L_o) can be explained by the fact that, in presence of NLI, the amplifier output power of the optimal design is smaller than in the (x_f, L_f) case, while the optimal x increases and noise factor improves, as reported in Fig. 3 for a 300-span link. Consequently, with an optimized EDFA we still have an improvement in AIR even if the BW is fixed, while with the (x_f, L_f) design AIR starts to shrink due to NLI, as shown in Fig. 2. Typically, we have 15% gain with (x_o, L_o) at 30 dBm pump power compared to the maximum AIR of the (x_f, L_f) case.

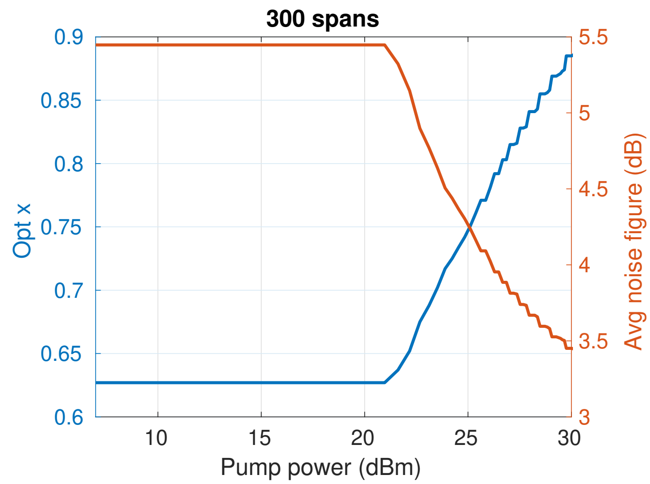

Figure 3. Optimal inversion (left axis) and average noise figure (right axis) versus pump power for a 300-span link.

In summary, when we fix the bandwidth, there is a unique optimum amplifier design when overlooking NLI. In presence of NLI, for pump powers below or equal to the NLT, this unique design enables to approach the optimum design AIR by less than 3% whatever the conditions of distance or NLC. An optimum design could enable to further increase the AIR by up to 15%, but at the expense of an increase of pump powers by more than 8 dB beyond the NLT. This means that in common submarine network applications, the "unique" design is quasi-optimal, and will become even better during the lifetime of a cable since the system NLT should naturally increase by using higher symbol rates channels with more and more efficient intra-channel NLT. Last, this "unique" design, follows a simple, affine, relationship between P_p and signal output power. Once this relationship is calibrated, this enables to perform quick system optimization studies without entering the details of the EDFA.

4.2 Variable Bandwidth ($\leq$ 5 THz)

Similarly to Figs. 1 and 2, Fig. 4 shows the PE and AIR versus P_p for a 100, 200 and 300-span link, for the variable BW case, with NLI and for the different strategies: (x_o, L_o) (solid), (x_o, L_f) (dashed) and (x_f, L_f) (dotted). The total WDM launch power at NLT for [100, 200, 300] spans are, respectively: [18.9, 18.5, 18.4] dBm, corresponding to [22.3, 21.8, 21.6] dBm of pump.

In this variable BW case, the values of (x_f, L_f) for [100, 200, 300] spans are respectively: [(0.627, 6.5 m), (0.638, 5.9 m), (0.640, 5.8 m)], yielding an optical bandwidth of [5.0, 4.8, 4.7] THz. We notice that even if the reference pump is the same, the optical BW obtained is not the same for the three distances. This is related to the BW dependence on SNR, set by the SNR-BW trade-off in AIR maximization, a topic that will be addressed later in this section.

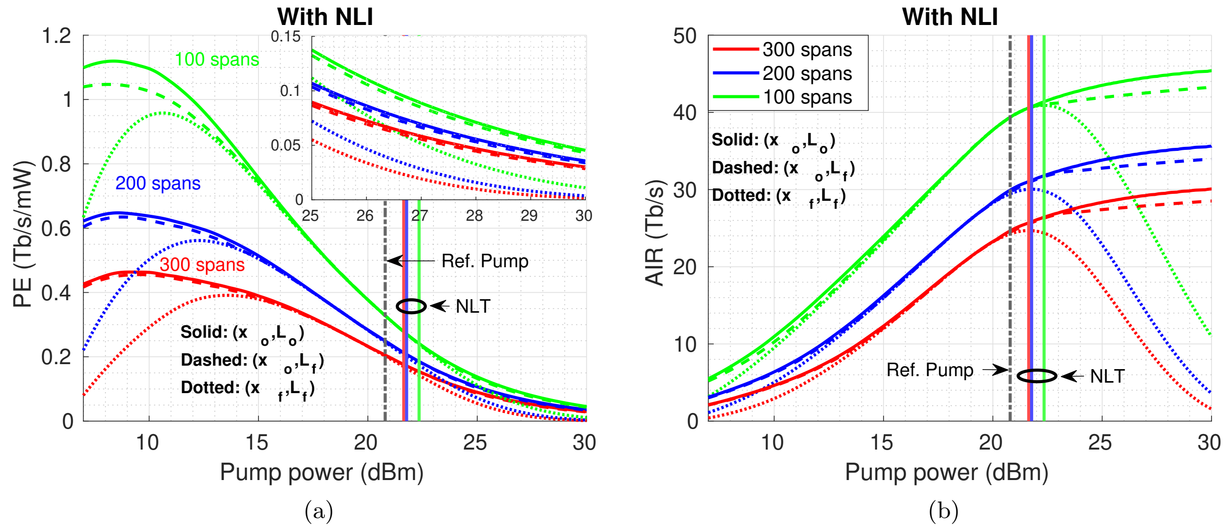

Figure 4. Power efficiency (a) and AIR (b) versus pump power for the different optimization strategies and distances, with a variable bandwidth in the C-band for a 100, 200 and 300-span link. Inset is a zoom of PE from 25 to 30 dBm pump power.

First, we see that the main impact of PE improvement comes from optimizing x, since fixed-length (x_o, L_f) and optimal (x_o, L_o) designs have close performance.

Next, we have a broad range of pump powers, which depends on the reference pump choice, where "classical" designs (x_f, L_f) and (x_o, L_f) are very close to optimal for all distances. From 14.2 to 21.8 dBm pump powers (about NLT - 8 to NLT for a 300-span link), operating with fixed parameters (hence fixed BW) still leads to a performance close to optimal within 5 % for all distances. More precisely, at NLT for [100, 200, 300] spans the gain in PE is respectively $[1.2, 3.7, 4.1]\%$ with 50% NLC. For comparison, the respective gain at the same pump power with NLC of 0% and 100% is: $[2.2, 5.3, 6.0]\%$ and $[0.2, 2.3, 2.4]\%$. Here, the gains in PE are higher than in the fixed-BW case, since the reference pump yielded smaller bandwidths ([5.0, 4.8, 4.7] THz) for the (x_f, L_f) design, while the optimum is at 5 THz.

However, as we drive out of this pump power range, optimizing the amplifier parameters starts to enable higher gains in PE/AIR. Above NLT, even if we compare the AIR enhancement using (x_o, L_o) to the AIR at NLT using (x_f, L_f), it continues to grow with pump power (as for the fixed bandwidth case) due to the increase of optimal inversion and the improvement of the noise figure while the optimum bandwidth grows up to 5 THz.

But contrarily to the fixed-BW case, for a variable BW we have a PE improvement using the optimal design even at low pumps: comparing the top PE of the (x_o, L_o) and (x_f, L_f) designs, we have gains of [16.8, 15.3, 18.5]% for [100, 200, 300] spans respectively. This is allowed by a small bandwidth in the low-pump regime, which can be explained by the fact that, from eq. (1), AIR maximization depends on the BW-SNR trade-off. Since AIR grows proportionally with the logarithm of the SNR, increasing the bandwidth is more efficient at high SNR. However, in the low-SNR regime, $\log_2(1 + \mathrm{SNR}) \sim \mathrm{SNR}$, so BW and SNR have the same importance in AIR maximization. More intuitive discussions about the BW-SNR trade-off is provided in Sec. 4.3.

Although at low pump powers the variable BW (x_o, L_o) design allows significant PE gains, still the number of fiber pairs for an energy-constrained subsea link considerably grows when compared to the (x_f, L_f) design, also increasing the system cost. For instance, for a 300-span link, the above-mentioned 18.5% gain in the corresponding top PE of the (x_o, L_o) versus (x_f, L_f) designs by reducing fiber pump power by 4.4 dB would result, for a submarine system constrained by a fixed total available pump power and a variable fiber count, in a 18.5% gain in cable AIR with the optimal design, provided fiber count is almost tripled. Hence, its feasibility in a limited power budget subsea system can be undermined by a techno-economics analysis, which the simple PE optimization did not consider.

4.3 Optimal BW Evolution

Here we discuss the evolution the optimal bandwidth with pump power and its relationship with SNR when maximizing AIR. Fig. 5 shows the optimal BW versus pump power for different distances in presence of NLI and without any constraints in the BW (can be outside the C-band defined) for better comprehension.

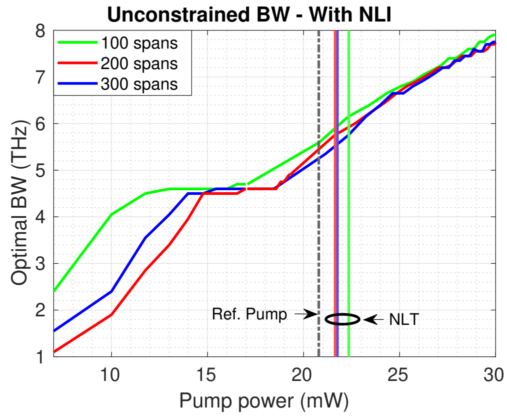

Figure 5. Optimal BW versus P_p for 300, 200 and 100 spans, with NLI, 50% NLC and unconstrained BW.

From the figure, we see that the optimal EDFA bandwidth is an increasing function of pump power. However, there is a range of pump powers where the optimum BW is constant around 4.6 THz. This means we can operate in this region with a fixed BW, hence simple (x_f, L_f) design, to obtain optimal performance, as discussed in the previous subsection.

The BW evolution with P_p depends on the BW weight compared to SNR's in AIR maximization. To better understand this trade-off, we show in Fig. 6 the bandwidth and SNR evolution with inversion at different pump powers, as done in Ref. 13, and in presence of NLI for a 300-span link. To better visualize this effect, the bandwidth is unconstrained. Compared to this work's results, the optimal inversion position on the BW vs. x curve would only change for Fig. 6(c) since we chop its maximum bandwidth at 5 THz. The optimal length used in each curve is reported in the figure and x_o is indicated by the magenta dots.

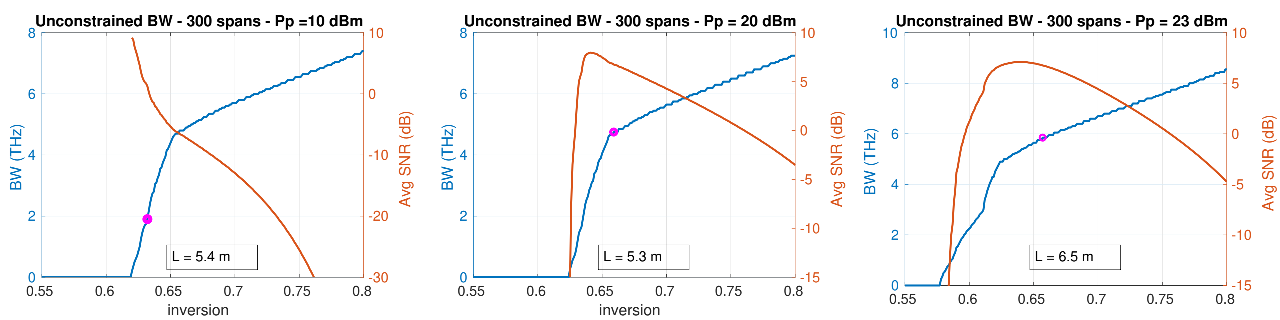

(a) (b) (c)

Figure 6. Bandwidth (left axis) and average SNR (right axis) versus inversion for a 300-span link. a) 10 dBm pump power. b) 20 dBm pump power. c) 23 dBm pump power.

From Fig. 6, we first see that the optimal BW increases with pump power: at 20 dBm, the x_o is found at the “knee” point of the curve BW vs. inversion (at the BW change of slope). At this point, SNR is not optimal, but AIR is maximized because BW has more importance in the SNR-BW trade-off. At low pumps, such as 10 dBm, the SNR regime is lower than in the previous case, so it has more weight in AIR maximization. Then BW will shrink in order to achieve a higher SNR. For high pumps, such as 23 dBm, x_o is not at the “knee” point either. In this case, NLI rises and optimal inversion shifts to higher values to increase BW and compensate the SNR degradation due to NLI. Again, the optimum is not found at top SNR because BW is more important for the trade-off in this regime. From this BW dependency with SNR, we also understand why the reference pump yields different bands for each distance: SNR of the 300-span link is lower, hence it has more importance in AIR optimization than BW compared to the 100-span link, which makes the the higher link to have a lower BW.

Another practical way to understand the shrinking of the optimal bandwidth at low pumps is to analyze the gain shape obtained when optimizing EDFA parameters. Fig. 7 reports the amplifier gain versus wavelength when using (x_o, L_o) at each pump power as in Fig. 6 with a variable BW within the C-band, for a 300-span link and including NLI. Horizontal line indicates the span loss A, at which the GSF will chop all gain above this level in order to keep a constant power after each amplifier. While the entire gain is shown in dotted lines, the useful gain (above A) is plotted in solid lines.

From the figure, we see that when the pump power is scarce (as 10 dBm), only the channels whose gain is close to A are allocated, so we do not need much power to amplify them. Besides, by not populating the entire C-band, the GSF gain chopping is smaller and wastes fewer of the very limited pump photons. On the other hand, at higher pumps, we have sufficient power so that all gain is above the attenuation level, allowing us to occupy the entire C-band. In this case, the GSF chops a larger amount of the EDFA gain, but the induced GSF power removal is acceptable since we have more pump power available than in the previous scenario.

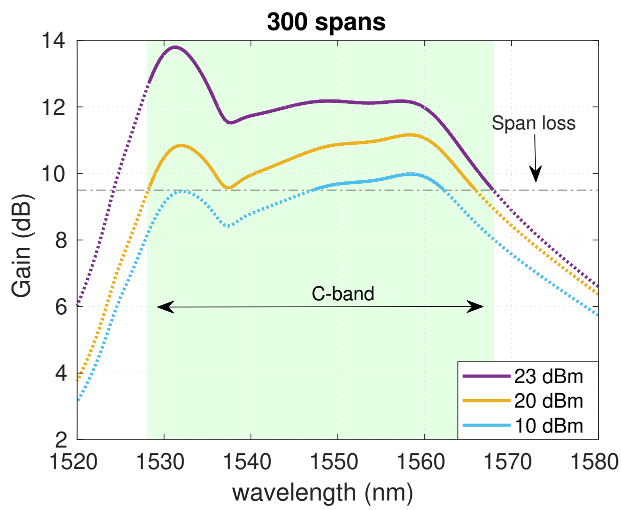

Figure 7. EDFA gain shape with optimized parameters at $P_p = 10$, 20 and 23 dBm for a 300-span link, with NLI and a variable BW within the C-band. For each pump, the parameters used are respectively: [(0.632, 5.4 m), (0.638, 5.9 m), (0.688, 5.4 m)].

4.4 ASE to NLI ratio

Here we discuss the impact of optimizing EDFA population inversion in the system's operating regime by analyzing the ASE to NLI power ratio. When the EDFA parameters are fixed, the "classical" NLT is defined by the launch WDM power at which AIR is maximized. At this operating point, the NLI power (P_{NLI}) is half of the ASE power (P_{ASE}).[19] However, when optimizing x at each pump power, the system operates in the linear regime, i.e., below the NLT. This is proven analytically in the Appendix B and, to illustrate it, Fig. 8(a) shows the ASE to NLI ratio versus P_p for a 300-span link for the optimal (x_o, L_o) (with variable BW within the C-band) and fixed-parameters (x_f, L_f) designs.

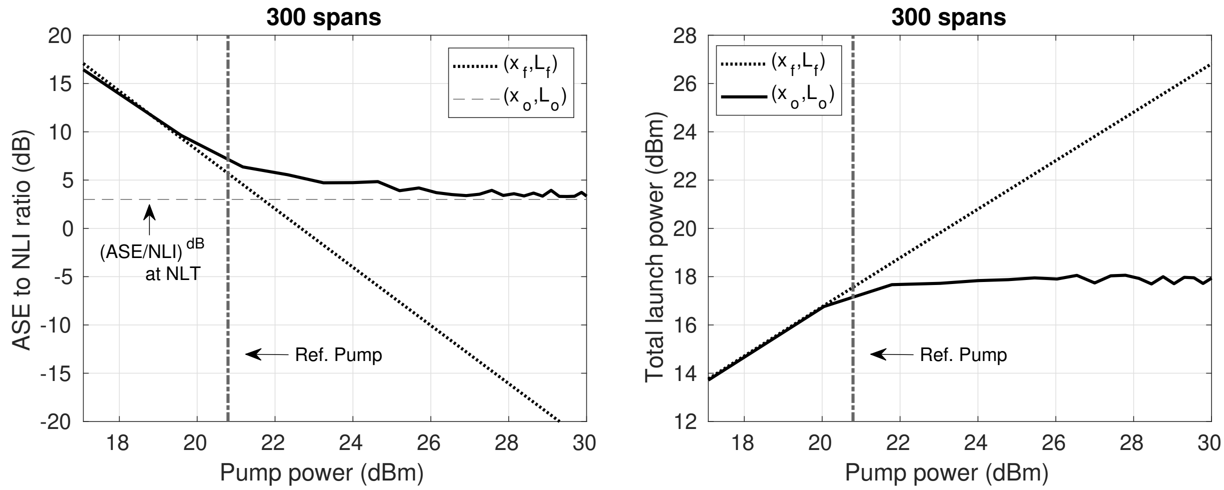

(a) (b)

Figure 8. a) ASE to NLI ratio b) Total launch power versus pump power for a 300-span link using optimal (solid) and fixed-parameters (dots) designs. NLC = 50%, variable BW in the C-band.

As discussed, when optimizing x in presence of NLI, it increases with pump power, improving the amplifier noise figure. In turn, the optimal launch power (which depends on inversion and pump power) saturates after a given pump, as shown in Fig. 8(b). Since ASE decreases and NLI keeps constant with pump power, SNR grows continuously and AIR does not reach a maximum, as opposed to the case where x is fixed as discussed previously. Moreover, the launch power saturates to a level where the ASE is still dominant over NLI, making the system to operate in linear regime. As Fig. 8(a) shows, the ASE to NLI ratio slowly decreases, but even at very high P_p (30 dBm), it still does not reach 3 dB for the optimal design.

5. CONCLUSION

We revisited the EDFA designs in subsea links by assessing their performance when optimizing amplifier settings such as population inversion, EDF length and optical bandwidth to maximize capacity. We also compared the optimal design (x_o, L_o) with more classical approaches: only length fixed (x_o, L_f) and both fixed (x_f, L_f). For a fully occupied C-band, we showed a unique EDFA design for all pump powers if NLI is not considered. When including it, the optimal strategy can improve PE as pump power increases, but it enables little gain at NLT (1.6% for a 300-span link). When allowing the BW to vary, we still have a broad region of pump powers where we can work with fixed parameters, hence with constant BW. This region is where typical submarine systems operate and is also convenient since we can use simple EDFA models, such as the affine law, to perform parametric studies. However, at very low pumps, we can have significant gains: we show a PE enhancement using (x_o, L_o) compared to (x_f, L_f) of up to 18.5 % at the top PE of each design. Although a variable BW with pump power yields better power efficiency than conventional fixed-parameters strategies, its application in subsea systems is arguable since it would need considerably more fiber pairs to achieve high capacities. Finally, we show analytically and provide an example that the system operates in a rather linear regime when optimizing the EDFA population inversion, even at high pump powers.

APPENDIX A. AFFINE LAW AND SALEH MODEL RELATION FOR CIP

We show here that, for the CIP allocation and when clamping the inversion, the EDFA Saleh model is equivalent to an affine law. Starting from the Saleh balance equation written in terms of power, we have:

$$\sum_{j=1}^{N_c} \frac{P_j^{in}}{hf_j}(G_j(x) - 1) = \frac{P_p}{hf_p}(1 - G_p(x)) - \frac{r_M}{\tau}x - Q_{ASE}^{F+B}(x) \tag{6}$$

where P_j^{in} is the j-th WDM channel power at the EDFA input. For the CIP case, signal power is independent of channel j, hence the total input power is simply $P_I = N_c \cdot P^{in}$. Then, Eq. (6) becomes:

$$P_I \sum_{j=1}^{N_c} \frac{(G_j(x)-1)}{hf_j} = N_c \left(\frac{P_p}{hf_p}(1-G_p(x)) - \frac{r_M}{\tau}x - Q_{ASE}^{F+B}(x) \right) \tag{7}$$

In turn, the amplifier total output power is $P_O = P_I \sum_{j=1}^{N_c} G_j$. Since the amplifier is followed by a gain flattening filter that chops the gain at the attenuation level A, we have: $P_O = P_I \cdot A$. Finally, we retrieve the affine law as well as the relationship of the EDFA optical-to-optical conversion efficiency and transparency pump with Saleh model parameters as reported in eqs. (4) and (5):

$$P_O(x) = \underbrace{\frac{N_c A \frac{(1-G_p(x))}{hf_p}}{\sum_{j=1}^{N_c} \dfrac{G_j(x)-1}{hf_j}}}_{\eta_{oo}} P_p - \underbrace{\frac{N_c A(\frac{r_M}{\tau}x - Q_{ASE}^{F+B}(x))}{\sum_{j=1}^{N_c} \dfrac{G_j(x)-1}{hf_j}}}_{\eta_{oo}\cdot P_{p0}} \tag{8}$$

where we define $P_{p0} \triangleq \dfrac{hf_p(\frac{r_M}{\tau}x - Q_{ASE}^{F+B}(x))}{1-G_p(x)}$.

APPENDIX B. LINEAR OPERATING REGIME WITH OPTIMUM INVERSION

We show here that a system works in linear regime when optimizing EDFA inversion. We first define an equivalent frequency-flat SNR_e that achieves the same AIR of eq. (1): $\mathrm{AIR} \triangleq 2BW(x)\log_2(1+\Gamma\mathrm{SNR}_e(x))$. Since we vary the EDFA inversion, its output power (hence SNR), bandwidth and noise figure are x-dependent. In the case of a constant input power allocation as we study here, we define also a WDM averaged NLI and ASE noise power generated at a single span: $\mathrm{NLI} = \sigma_{nl,1}^2(x) =< a_{nl,j} > P_e^3(x) = a_{nl}P_e^3(x)$ and $\mathrm{ASE} = \sigma_{ase,1}^2(x) \triangleq < k_j F_j(x) >= k_e F_e(x)$, where $< . >$ denotes frequency averaging, $a_{nl,j}$ is the NLI coefficient defined in Ref. 14, $k_j = hf_j \Delta f A$ and $P_e(x)$ is the signal power per channel. From the generalized droop formula, we have that: $\mathrm{SNR}_e(x) = \frac{1}{\chi_e^{-M}(x)-1}$, where $\chi_e^{-1}(x) = 1 + a_{nl}P_e^2(x) + \frac{k_e F_e(x)}{P_e(x)}$. At a given pump power, we search for the inversion that maximizes AIR. Hence, setting its total derivative to zero:

$$\begin{aligned} &\frac{2}{\ln 2} P_e^2(x) \ln(1+\Gamma\mathrm{SNR}_e(x)) \cdot BW'(x) + \frac{2BW(x)}{\ln 2}\left(\frac{1}{1+\Gamma\mathrm{SNR}_e(x)}\right)\cdot(-\Gamma\mathrm{SNR}_e^2(x))\cdot \\ &\qquad M\cdot\chi_e(x)^{-M+1}\cdot\left(P_e'(x)\left(\underbrace{2a_{nl}P_e^3(x) - k_eF_e(x)}_{\text{2 NLI - ASE}}\right) + k_eP_e(x)F_e'(x)\right) = 0 \end{aligned} \tag{9}$$

Isolating the term 2 NLI - ASE:

$$\text{2NLI - ASE} = \frac{P_e^2(x)\ln(1+\Gamma\mathrm{SNR}_e(x))}{\left(\dfrac{BW(x)}{1+\Gamma SNR_e(x)}\right)\Gamma SNR_e^2(x)\cdot M\cdot\chi_e(x)^{-M+1}} \cdot \frac{BW'(x)}{P_e'(x)} - k_eP_e(x)\frac{F_e'(x)}{P_e'(x)} \triangleq C \tag{10}$$

$$\text{NLI} = \frac{\text{ASE + C}}{2} \tag{11}$$

Now, to determine the system operating point, we analyze the sign of C: noise figure $F(x)$ decreases with inversion, because of the spontaneous emission factor definition. At a fixed pump, the signal power per channel

$P(x)$ also decreases with inversion because of the Saleh constraint. Hence $\frac{F'(x)}{P'(x)} > 0$. Because the EDFA gain grows with x, so does the number of channels where $G_j > A$, and consequently BW increases. Hence $\frac{BW'(x)}{P'(x)} < 0$. Besides, the term multiplying $\frac{BW'(x)}{P'(x)}$ as well as k are also positive, since they depend on positive physical parameters. Therefore, C is always negative and from eq. (11) NLI $< \frac{\text{ASE}}{2}$, so we are still below the NLT, hence in the linear regime.

REFERENCES

[1] Winzer, P. J., "Capacity scaling through spatial parallelism: From subsea cables to short-reach optical links," in [*2021 Optical Fiber Communications Conference and Exhibition (OFC)*], 1–1 (2021).

[2] Pecci, P., Jovanovski, L., Barezzani, M., Kamalov, V., Marcerou, J., Cantono, M., Gumier, M., Courtois, O., and Vusirikala, V., "Pump farming as enabling factor to increase subsea cable capacity," in [*SubOptic*], 1–7 (2019).

[3] Frisch, T. and Desbruslais, S., "Electrical power, a potential limit to cable capacity," in [*SubOptic*], (2013).

[4] Sinkin, O. V., Turukhin, A. V., Sun, Y., Batshon, H. G., Mazurczyk, M. V., Davidson, C. R., Cai, J.-X., Patterson, W. W., Bolshtyansky, M. A., Foursa, D. G., and Pilipetskii, A. N., "Sdm for power-efficient undersea transmission," *J. Lightwave Technol.* **36**, 361–371 (Jan 2018).

[5] Srinivas, H., Downie, J. D., Hurley, J., Liang, X., Himmelreich, J., Perin, J. K., Mello, D. A. A., and Kahn, J. M., "Modeling and experimental measurement of power efficiency for power-limited sdm submarine transmission systems," *Journal of Lightwave Technology* **39**(8), 2376–2386 (2021).

[6] Antona, J.-C., Carbo-Meseguer, A., and Letellier, V., "Evolution of high capacity submarine open cables," in [*2019 Asia Communications and Photonics Conference (ACP)*], 1–3 (2019).

[7] Downie, J. D., Liang, X., and Sterlingov, P., "Power efficiency in submarine systems using various capacity metrics," in [*2021 Optical Fiber Communications Conference and Exhibition (OFC)*], 1–3 (2021).

[8] Bononi, A., Antona, J.-C., Serena, P., Carbo-Meseguer, A., and Lasagni, C., "The generalized droop model for submarine fiber-optic systems," *Journal of Lightwave Technology* **39**(16), 5248–5257 (2021).

[9] Antona, J.-C., Meseguer, A. C., and Letellier, V., "Transmission systems with constant output power amplifiers at low snr values: A generalized droop model," in [*2019 Optical Fiber Communications Conference and Exhibition (OFC)*], 1–3 (2019).

[10] Bononi, A., Antona, J.-C., Lonardi, M., Carbo-Meseguer, A., and Serena, P., "The generalized droop formula for low signal to noise ratio optical links," *Journal of Lightwave Technology* **38**(8), 2201–2213 (2020).

[11] Perin, J. K., Kahn, J. M., Downie, J. D., Hurley, J., and Bennett, K., "Importance of amplifier physics in maximizing the capacity of submarine links," *Journal of Lightwave Technology* **37**(9), 2076–2085 (2019).

[12] Cho, J., Raybon, G., Burrows, E., Antona, J.-C., Fontaine, N., Ryf, R., Chen, H., Chandrasekhar, S., Sula, E., Olsson, S., Grubb, S., and Winzer, P., "Optimizing gain shaping filters with neural networks for maximum cable capacity under electrical power constraints," in [*2020 European Conference on Optical Communications (ECOC)*], 1–4 (2020).

[13] Bononi, A., Serena, P., and Antona, J.-C., "A state-variable approach to submarine links capacity optimization," *Journal of Lightwave Technology* **39**(18), 5753–5765 (2021).

[14] Bononi, A., de Araujo, J. T., Lasagni, C., Serena, P., and Antona, J.-C., "The constant power spectral density model for capacity optimization of submarine links," *Journal of Lightwave Technology* , 1–11 (2022).

[15] Poggiolini, P., Bosco, G., Carena, A., Curri, V., Jiang, Y., and Forghieri, F., "The gn-model of fiber non-linear propagation and its applications," *Journal of Lightwave Technology* **32**(4), 694–721 (2014).

[16] Georges, T. and Delevaque, E., "Analytic modeling of high-gain erbium-doped fiber amplifiers," *Opt. Lett.* **17**, 1113–1115 (Aug 1992).

[17] Giles, C. and Desurvire, E., "Propagation of signal and noise in concatenated erbium-doped fiber optical amplifiers," *Journal of Lightwave Technology* **9**(2), 147–154 (1991).

[18] Carbo, A. M., Pacheco, J. L. d. O., Antona, J.-C., de Araujo, J. T., and Letellier, V., "Multi-core vs hollow-core fibers: Technical study of their viability in sdm power-constraint submarine systems," in [*European Conference on Optical Communications (ECOC)*], 1–3 (2022).

[19] Bosco, G., Carena, A., Cigliutti, R., Curri, V., Poggiolini, P., and Forghieri, F., "Performance prediction for wdm pm-qpsk transmission over uncompensated links," in [*2011 Optical Fiber Communication Conference and Exposition and the National Fiber Optic Engineers Conference*], 1–3 (2011).